SLAC-PUB-2762
June 1981
(T/E)

EXCLUSIVE PROCESSES IN QUANTUM CHROMODYNAMICS*

Stanley J. Brodsky
Stanford Linear Accelerator Center
Stanford University, Stanford, California 94305

and

G. Peter Lepage†
Laboratory of Nuclear Studies
Cornell University, Ithaca, New York 14853

ABSTRACT

Large momentum transfer exclusive processes and the short distance structure of hadronic wave functions can be systematically analyzed within the context of perturbative QCD. We review predictions for meson form factors, two-photon processes $\gamma\gamma \to M\bar{M}$, hadronic decays of heavy quark systems, and a number of other related QCD phenomena.

I. INTRODUCTION

One reason why detailed, quantitative tests of quantum chromodynamics[1] are so difficult is that measurements of basic quark and gluon subprocesses must be done within the confines of hadrons. Fortunately, it is often possible to isolate the largely unknown bound state hadron dynamics in terms of process-independent probability distributions and amplitudes. The predictions for both inclusive[1] and exclusive[2-5] reactions which involve large momentum transfer can then be factorized into hard-scattering quark and gluon subprocess amplitudes, T_H, representing the short distance physics, convoluted with evolved distribution functions or amplitudes containing the long distance dynamics.

As we shall discuss in this talk, large momentum transfer exclusive reactions such as elastic lepton-hadron, photon-hadron and hadron-hadron scattering can provide an extensive, experimentally accessible, and perhaps definitive testing ground for perturbative QCD.[6] In particular, the power-law behavior of these reactions directly tests the scale-invariance of the basic quark and gluon interactions at short distances, as well as the SU(3)-color symmetry of the hadronic valence wave functions. The normalizations of the exclusive amplitudes (both relative and absolute) test the basic

---

* Work supported by the Department of Energy under contract DE-AC03-76SF00515.
† Work supported by the National Science Foundation.

(Invited talk presented at the Conference on Perturbative QCD at Florida State University, Tallahassee, March 25-28, 1981.)

flavor and spin symmetry structure of the theory as well as the asymptotic boundary condition for meson valence state wave functions obtained from the meson leptonic decay rates. The angular variation, helicity structure, and absolute sign of exclusive amplitudes test the spin and bare couplings of quarks and gluons. In addition the predicted logarithmic modifications of exclusive amplitudes reflect the asymptotic freedom variation of the running coupling constant and the singularities in the operator product expansion of hadronic wave functions at short distances. In the case of exclusive processes such as meson form factors and the two-photon reactions $\gamma\gamma \to M\bar{M}$, the derivations can be carried out with the same degree of rigor as that for the QCD predictions for structure function moments. An implicit assumption of all such analyses is that the short distance behavior of any nonperturbative or confinement dynamics is more regular than that given order-by-order in perturbation theory.[7]

A convenient representation[8] of a hadronic bound state in terms of quark and gluon constituents is the set of Fock state wave functions $\psi^{(n)}$ as defined at equal time $\tau = z + t$ on the light-cone. We will choose the physical gauge $A^+ = A^0 + A^3 = 0$. By using light-cone quantitization (or equivalently, infinite-momentum-frame methods), we can define charge and number operators which are diagonal in the Fock state basis, i.e., conserved quantities which do not change particle number. The amplitude to find n (on-mass-shell) quarks and gluons in a hadron with 4-momentum P^μ directed along the z-direction and spin projection S_z is defined as ($k^\pm = k^0 \pm k^3$)

$$\psi^{(n)}_{S_z}\left(x_i, \vec{k}_{\perp i}, s_i\right) \quad , \qquad x_i \equiv \frac{k_i^+}{P^+} \quad ,$$

where by momentum conservation $\sum_{i=1}^{n} x_i = 1$ and $\sum_{i=1}^{n} \vec{k}_{\perp i} = 0$. The s_i specify the spin-projection of the constituents. The state is off the light-cone energy shell,

$$P^- - \sum_{i=1}^{n} k_i^- = \frac{M^2 - \sum_{i=1}^{n} \frac{\vec{k}^2_{\perp i} + m_i^2}{x_i}}{P^+} < 0 \quad . \qquad (1.1)$$

The valence Fock states (which in fact dominate large momentum transfer exclusive reactions) are the $|q\bar{q}\rangle$ ($n = 2$) and $|qqq\rangle$ ($n = 3$) components of the meson and baryon. For each fermion or anti-fermion constituent $\psi^{(n)}_{S_z}(k_{\perp i}, x_i, s_i)$ multiplies the spin factor $u(\vec{k}_i)/\sqrt{k_i^+}$ or $v(\vec{k}_i)/\sqrt{k_i^+}$. The wave function normalization condition is

$$\sum_{(n)(s_i)} \int \left|\psi^{(n)}_{S_z}\left(k_{\perp i}, x_i, s_i\right)\right|^2 \left[d^2k_\perp\right]\left[dx\right] = 1, \qquad (1.2)$$

where

$$\left[d^2k_\perp\right] \equiv 16\pi^3\,\delta^{(2)}\left(\sum_i k_{\perp i}\right)\prod_{i=1}^{n}\frac{d^2k_{\perp i}}{16\pi^3} \quad ,$$

and

$$\left[dx\right] = \delta\left(1-\sum_i^n x_i\right)\prod_{i=1}^{n} dx_i \quad .$$

By studying the wave functions themselves, one could in principle understand not only the origin of the standard structure functions, but also the nature of multi-particle longitudinal and transverse momentum distributions, helicity dependences, as well as the effects of coherence. For example, the standard quark and gluon structure functions (probability distributions) which control large momentum transfer inclusive reactions at the scale Q^2 are

$$G_{a/H}(x_a,Q) \equiv d_a^{-1}(Q^2)\sum_{n,s_i,S_z}\int^{k_{\perp a}^2<Q^2}\left|\psi^{(n)}_{S_z}(k_{\perp i},x_i,s_i)\right|^2\left[d^2k_\perp\right]\left[dx\right] \times \delta\left(x-x_a\right) \quad , \qquad (1.3)$$

where $d_a^{-1}(Q^2)$ is due to the wave function renormalization of the constituent a. Note that only terms which fall-off as $|\psi|^2 \sim (k_{\perp a}^2)^{-1}$ (modulo logs) contribute to the Q^2 dependence of the integral. These contributions are analyzable by the renormalization group and correspond in perturbative QCD to quark or gluon pair production or fragmentation processes associated with the struck constituent a. In general, unless x is close to 1, all Fock states in the hadron contribute to $G_{a/H}$. [Multi-particle probability distributions are simple generalizations of Eq. (1.3).] Inclusive cross sections for reactions such as deep inelastic lepton or photon scattering can then be obtained by convoluting $G_{a/H}(x,\tilde{Q})$ with the elementary hard scattering quark or gluon subprocess cross sections $d\hat{\sigma}_a$ computed for on-shell constituents (a) collinear with hadron H. The scale $\tilde{Q}$ is controlled by the momentum transfer in the subprocess and the available phase-space for the spectator constituents. A detailed discussion is given in Ref. 9.

In the next sections we shall show how exclusive processes in QCD can be directly related to the valence Fock states $\psi_{q\bar{q}}$ and ψ_{qqq} for mesons and baryons.

II. CALCULATIONS OF QCD EXCLUSIVE PROCESSES

The simplest illustration of the calculation of exclusive reactions in QCD is the evaluation of the $F_{\pi\gamma}(Q^2)$, $\gamma \to \pi^o$ transition form factor, which is measureable in two-photon $ee \to ee\pi^o$ ($\gamma^*\gamma \to \pi^o$) reactions [see Fig. 1(a)]. The form factor is defined via the amplitude

$$\Gamma^\mu = -ie^2 F_{\pi\gamma}(Q^2)\, \epsilon^{\mu\nu\rho\sigma}\, p^\pi_\nu\, \epsilon_\rho\, q_\sigma \quad . \tag{2.1}$$

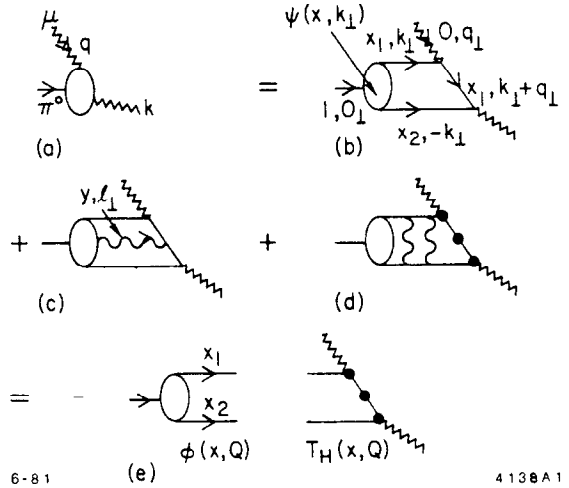

Fig. 1. Perturbative QCD analysis of the $\gamma\gamma^* \to \pi^o$ amplitude. Higher Fock state contributions such as (c) are power-law suppressed in a physical gauge. The factorization of $F_{\pi\gamma}(Q^2)$ is shown in (d).

The lowest order contribution is shown in Fig. 1(b). We choose a frame with

$$q = \left(q^+, q^-, \vec{q}_\perp\right) = \left(0, 2p\cdot q/p^+, q_\perp\right) \quad , \quad q_\perp^2 = Q^2 = -q^2 \quad ,$$

$$p^\pi = \left(p^+, p^-, \vec{p}_\perp\right) = \left(p^+, M^2/p^+, \vec{0}_\perp\right) \quad . \tag{2.2}$$

We then compute the $\gamma^*\gamma \to \pi^o$ amplitude in time-order perturbation theory in terms of the light-wave Fock state amplitude:

$$\psi\left(x, \vec{k}_\perp\right) = \text{F.T.} \left\langle 0 \left| T\, \bar{\psi}\left(\frac{z}{2}\right) \psi\left(-\frac{z}{2}\right) \right| \pi \right\rangle \Big|_{z^+ = 0} \quad . \tag{2.3}$$

The denominator associated with the fermion propagator is proportional to $(k_\perp + x_1 q_\perp)^2$. For large Q^2 one then easily finds ($x_1 + x_2 = 1$)

$$F_{\pi\gamma}(Q^2) = \frac{2\sqrt{n_c}\left(e_u^2 - e_d^2\right)}{Q^2} \int_0^1 \frac{dx}{x_1 x_2} \int^{k_\perp^2 < \tilde{Q}^2} \frac{d^2k_\perp}{16\pi^2}\, \psi\left(x, k_\perp\right), \tag{2.4}$$

where

$$\tilde{Q} = \left(\min_{i=1,2} x_i \right) Q \quad .$$

The QCD radiative corrections to this result can be organized in the following way: First consider the loop integration $(\vec{\ell}_\perp, y)$ associated with gluons which attach to the exchanged fermion [Figs. 1(c) and 1(d)]. For the ultraviolet region $\ell_\perp > \tilde{Q}$ the vertex and self-energy insertions lead to the fermion line renormalization factor $d_F^{-1}(\tilde{Q}^2)$. For $\ell_\perp < Q$, one obtains either higher corrections in $\alpha_s(\tilde{Q}^2)$ to the $q\bar{q} + \gamma^* \to \gamma$ amplitude or in the case of Fig. 1(c), power-law suppressed contributions (in $A^+ = 0$ gauge). The gluons which are exchanged between the quark legs are included in the definition of $\psi(x,\vec{k}_\perp)$ and lead to a power-law tail $\psi(x,\vec{k}_\perp) \sim k_\perp^{-2}$. This implies a logarithmic Q^2 dependence for the (gauge-independent) "distribution amplitude"

$$\phi(x,Q) \equiv d_F^{-1}(Q) \int^{k_\perp^2 < Q^2} \frac{d^2k_\perp}{16\pi^3} \psi\left(x,k_\perp\right) \quad . \tag{2.5}$$

Since $z^+ = 0$, $z^2 = -z_\perp^2 \sim \mathcal{O}(1/Q_\perp^2)$, and one can compute the Q^2 dependence of ϕ from the operator product expansion of $\bar{\psi}(z/2)\psi(-z/2)$ in Eq. (2.3) near the light-cone[10] to leading order in α_s:

$$\phi(x,Q) = x_1 x_2 \sum_{n=0}^{\infty} \left(\ell n \frac{Q^2}{\Lambda^2} \right)^{-\gamma_n} a_n \, C_n^{3/2}\left(x_1 - x_2\right) \quad , \tag{2.6}$$

where the γ_n are the standard nonsinglet anomalous dimensions. Alternatively, this result can be obtained via an evolution equation of the form[2]

$$Q^2 \frac{\partial}{\partial Q^2} \phi(x,Q) = \frac{\alpha_s(Q^2)}{4\pi} \int_0^1 dy \; V(x,y) \, \phi(y,Q) \tag{2.7}$$

where $V(x,y)$ is computed from the single gluon exchange kernel. We thus obtain

$$\begin{aligned} F_{\pi\gamma}(Q^2) &= \frac{2}{\sqrt{3}\, Q^2} \int_0^1 \frac{dx}{x_1 x_2} \, \phi(x,\tilde{Q}) \\ &= \frac{2\sqrt{n_c}\left(e_u^2 - e_d^2\right)}{Q^2} \sum_{n=0,2} a_n \left(\ell n \frac{Q^2}{\Lambda^2} \right)^{-\gamma_n} \end{aligned} \tag{2.8}$$

with corrections of order $\alpha_s(Q^2)$ and m^2/Q^2. The decay $\pi \to \mu\nu$ determines the wave function at the origin:

$$\frac{a_0}{6} = \int_0^1 dx\ \phi_\pi(x,Q) = \frac{f_\pi}{2\sqrt{3}} \quad . \tag{2.9}$$

In the case of the pion form factor, a similar analysis gives[2-5] (see Fig. 2):

$$F_\pi(Q^2) = \frac{16\pi\alpha_s(Q^2)}{3Q^2} \int_0^1 dx \int_0^1 dy\ \frac{\phi\left(x,\tilde{Q}_x\right)\phi\left(y,\tilde{Q}_y\right)}{x(1-x)\ y(1-y)} \quad . \tag{2.10}$$

Again to leading order in $\alpha_s(Q^2)$ and m^2/Q^2.

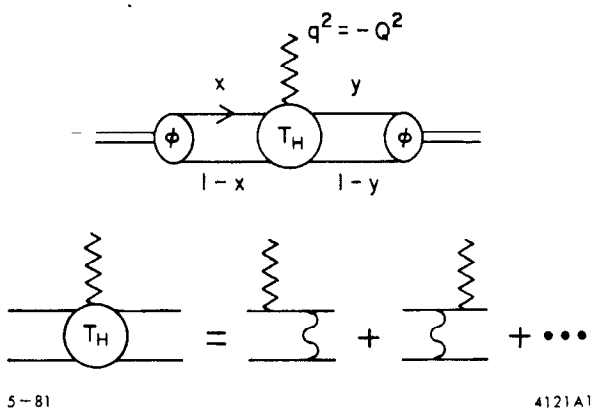

Fig. 2. Factorized structure and leading QCD contributions for the pion form factor in QCD.

Figure 3 illustrates this QCD prediction for Q^2F_π given 3 different initial functions $\phi(x,Q_0)$ at $Q_0^2 = 2\ \text{GeV}^2$ with representative values of the QCD scale parameter Λ^2. In each case the normalization is uniquely determined by (2.9); all curves ultimately converge to the asymptotic limit $Q^2F_\pi \to 16\pi\alpha_s(Q^2)f_\pi^2$.[5] For Fig. 3, we have multiplied (2.10) by $(1+m_\rho^2/Q^2)^{-1}$ to allow a smooth connection with the low Q^2 behavior suggested by vector dominance models.

The behavior exhibited in Fig. 3 can be radically modified if $\phi(x_i,Q_0)$ has nodes or other complex structure in x_i. However such behavior is unlikely for ground state mesons such as the pion. For these, one intuitively expects a smooth, positive-definite distribution amplitude, peaked about $x_1,x_2 \sim 1/2$. Given these constraints, the normalization of $F_\pi(Q^2)$ is largely determined by the breadth of the distribution -- broad distributions [Fig. 3(c)] result in a large form factor, narrow distributions [Fig. 3(b)] in a small one. The magnitude of the form factor also depends to some extent upon the scale parameter Λ^2 through the factor $\alpha_s(Q^2)$ in (2.10).

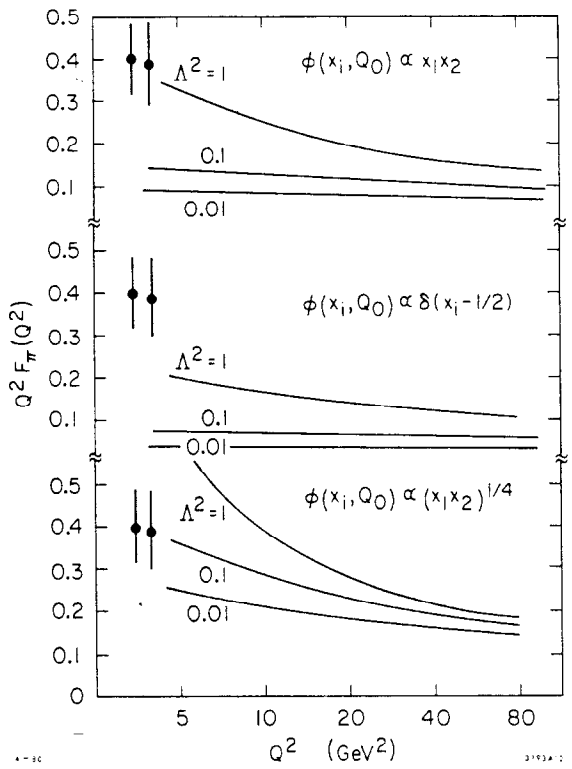

Fig. 3. Leading order QCD predictions for the pion form factor assuming various distribution amplitudes $\phi(x_i,Q_0)$ at $Q_0^2 = 2$ GeV^2 and various values of the QCD scale parameter Λ^2. The data are from the analysis of electroproduction $e^- p \to e^- + \pi^+ + n$; C. Bebek et al., Ref. 41.

An important question is the magnitude of the higher-order corrections to $F_\pi(Q^2)$. Since the gluon carries momentum transfer $-t \cong (1-x)(1-y)Q^2$, one expects that higher corrections will be minimized if one takes the argument of α_s in Eq. (2.10) to be a fraction $\lesssim 1/4$ of Q^2. A detailed calculation of the α_s correction has been recently given by R. D. Field, R. Gupta, S. Otto, and L. Chang,[11] with, however, the extra restriction that $\phi(x,Q) \equiv \sqrt{3}\, f_\pi\, x(1-x)$. Their result can be written (in the $\overline{\text{MS}}$ scheme) as:

$$Q^2 F_\pi(Q^2) = 0.43\, \alpha_s(\hat{Q}^2)\left[1 + 0.11\, \alpha_s + \ldots\right] \qquad (2.11)$$

with $\alpha_s(\hat{Q}^2) = \alpha_s(Q^2/16)$.

The complete calculation to this order also requires an evaluation of the order α_s corrections to the distribution amplitude. A detailed calculation may be possible by analyzing the breakdown of conformal invariance due to the Q^2-dependence of the kernel in the evolution equation.[12]

Unlike the electromagnetic form factor $F_\pi(Q^2)$, the $\gamma \to \pi^0$ form factor in leading order has no explicit dependence on $\alpha_s(Q^2)$. Consequently an accurate measurement of $F_{\pi\gamma}(Q^2)$ determines $\int_0^1 dx \left[\phi_\pi^*(x,\tilde{Q})/x(1-x)\right]$. This can be combined with the normalizing sum rule[13] [Eq. (2.9)] to constrain the x-dependence of $\phi_\pi(x,\tilde{Q})$. To illustrate this, consider normalized distribution amplitudes of the

general form

$$\phi_\pi(x,\tilde{Q}) = \frac{f_\pi}{2\sqrt{3}} \frac{\Gamma(2\eta+2)}{\left(\Gamma(\eta+1)\right)^2} (1-x)^\eta x^\eta \quad ; \quad \eta > 0 \qquad (2.12)$$

where large $\eta(\tilde{Q})$ implies a sharply peaked (at $x = 1/2$) distribution and small $\eta(\tilde{Q})$ gives a broad distribution. This ansatz gives a $\pi\gamma$ transition form factor

$$Q^2 F_{\pi\gamma}(Q^2) = 2f_\pi \frac{2\eta+1}{3\eta} \qquad (2.13)$$

which is clearly quite sensitive to the parameter η. For very high Q^2, $\eta(Q) \to 1$ and thus[2]

$$F_{\pi\gamma} \to \frac{2f_\pi}{Q^2} \quad \text{as} \quad Q^2 \to \infty \quad . \qquad (2.14)$$

The x-dependence of the integrand in Eq. (2.8) is identical to that in Eq. (2.10) for $F_\pi(Q^2)$. Consequently all dependence on ϕ_π can be removed by comparing the two processes. In fact, a measurement of each provides a direct determination of $\alpha_s(Q^2)$:[2]

$$\alpha_s(Q^2) = \frac{1}{4\pi} \frac{F_\pi(Q^2)}{Q^2 \left| F_{\pi\gamma}(Q^2) \right|^2} + O\left(\alpha_s^2\right) \quad . \qquad (2.15)$$

Once the $O(\alpha_s^2)$ corrections have been computed, this could be used to measure α_s and the QCD scale parameter Λ for a given renormalization prescription.

Of course all of these formulae are valid only at large Q^2; $O(m^2/Q^2)$ corrections become important at lower Q^2. However the $Q^2 \to 0$ behavior of $F_{\pi\gamma}$ is fixed by the experimental rates for the decay $\pi^0 \to 2\gamma$, or, equivalently as it turns out, by current algebra which implies:

$$F_{\pi\gamma}(Q^2) \to \frac{1}{4\pi^2 f_\pi} \quad \text{as} \quad Q^2 \to 0 \quad . \qquad (2.16)$$

To estimate the effects due to $O(m^2/Q^2)$ corrections, we write $F_{\pi\gamma}$ in terms of a monopole form

$$F_{\pi\gamma} \sim \frac{1}{4\pi^2 f_\pi} \frac{1}{1+\left(Q^2/8\pi^2 f_\pi^2\right)} \sim \frac{0.27\ \text{GeV}^{-1}}{1+Q^2/M^2} \qquad (2.17)$$

$$\left(M^2 \sim .68\ \text{GeV}^2\right)$$

which interpolates between the $Q^2 = 0$ and $Q^2 = \infty$ limits. The mass scale M^2 is quite similar to that measured for $F_\pi(Q^2)$. If the best $\eta(Q)$ in Eq. (2.12) is appreciably different from $\eta = 1$ at current Q^2, this mass-scale parameter might actually be more like

$$M^2(\eta) = .68\ \text{GeV}^2\ \frac{2\eta+1}{3\eta} \quad . \qquad (2.18)$$

Predictions for other meson form factors are given in Refs. 2 and 13.

These meson form factor results can also be derived using renormalization group methods, as has been shown by Mueller and Duncan.[4] The essential method is to prove Callan-Symansik equations for moments of the reducible quark scattering amplitudes. The evolution equation method and the renormalization group methods are equivalent, differing only in the organization of the calculation. The light-cone perturbation theory Fock-state methods, however, have a number of advantages: (a) direct calculation in the physical momentum-space $k_\perp$ and x variables; (b) simple connections between the Bethe-Salpeter wave functions, distribution amplitudes, and Fock state amplitudes; and (c) straightforward analyses of higher Fock states. Finally, we emphasize that the distribution amplitudes $\phi_M(x,Q)$ and $\phi_B(x_i,Q)$ are physical, gauge-invariant measures of the meson and baryon wave functions at short distances.[2]

III. LARGE MOMENTUM TRANSFER EXCLUSIVE PROCESSES IN QCD

Let us now briefly review the essential points for calculating an exclusive large momentum transfer hadronic amplitude in QCD. Away from possible special points in the x_i integrations (see below), a general hadronic amplitude $\mathcal{M}_{AB\to CD}(Q^2,\theta_{c.m.})$ can be written as a convolution over the x_i of a connected hard-scattering amplitude $T_H(x_i,s_i;Q^2,\theta_{c.m.})$ with the valence quark distribution amplitudes:[2]

$$\phi_M(x,\tilde{Q}) = d_F^{-1}(\tilde{Q}) \int^{k_\perp^2 < \tilde{Q}^2} d^2k_\perp\ \psi_{q\bar{q}}\left(x,k_\perp\right) \qquad (3.1)$$

and

$$\phi_B(x_i,\tilde{Q}) = d_F^{-3/2}(\tilde{Q}) \int^{k_{\perp i}^2 < Q^2} [d^2k_\perp]\psi_{qqq}(x_i,k_{\perp i}) \ , \ i = 1,2,3 \qquad (3.2)$$

for flavor singlet mesons and baryons, respectively. The pion form factor, for example, is given by[2-4] (see Fig. 2)

$$F_\pi(Q^2) = \int_0^1 dx \int_0^1 dy \ \phi_\pi^*(y,\tilde{Q}_y)\, T_H(x,y;Q^2)\, \phi_\pi(x,\tilde{Q}_x) \qquad (3.3)$$

where $\tilde{Q}_x = \min(x,1-x)Q$.

In T_H each hadron is replaced by massless, collinear valence partons, each carrying some fraction of the hadron's momentum. Thus T_H is the scattering amplitude for the constituents. The distribution amplitude $\phi_\pi(x,Q)$, for example, is the amplitude for finding a quark and antiquark in a pion carrying momentum fractions x and 1-x, respectively, and collinear up to the scale Q. The distribution amplitudes are weakly (logarithmically) Q-dependent due to QCD scaling violation. The detailed dependence can be derived via evolution equations[2] or the operator product expansion at short distances.[10]

The essential behavior of an exclusive amplitude at large Q^2 is determined by T_H. For most x_i, all internal quark and gluon legs are far off-shell [$p_j^2 \sim \tilde{Q}^2$, where $\tilde{Q}^2$ is a linear function of Q^2 and the x_i] in the lowest-order tree graphs for T_H. This is essential if contributions $k_\perp^2 << Q^2$ are to factorize, and thereby be absorbed into the distribution amplitudes. In higher orders T_H is defined to be "collinear irreducible"; i.e., the transverse momentum integrations are restricted to $k_\perp^2 > \tilde{Q}^2$ since the region $k_\perp^2 < \tilde{Q}^2$ is already included in ϕ. In general there can be endpoint regions of integration ($x_i \to 0$) and/or pinch (Landshoff) singularities[14] at particular values of x_i for which intermediate propagators in the connected quark scattering amplitude approach the mass shell, and factorization is jeopardized. In the case of the meson form factors, and amplitudes such as $\gamma\gamma \to M\bar{M}$, $\gamma^* + \gamma \to M$, and $e^+e^- \to M_1 \ldots M_N$ at fixed angle,[16] these regions of integration lead to power-law suppressed contributions, even at the tree level. We then can obtain rigorous predictions for these large momentum transfer processes; in particular T_H has a consistent perturbative expansion in $\alpha_s(Q^2)$.

For baryon form factors,[2,17] it is easily seen that any anomalous contribution from the endpoint region $x_1 \sim 1$, $x_2, x_3 \sim O(m/Q)$ is strongly suppressed by the Sudakov form factor which arises from the loop corrections to the near on-shell, high Q^2, $\bar{q}\gamma q$ vertex. The leading contribution to the baryon form factor thus comes from the hard scattering region. The Sudakov suppression of the endpoint region implies an all orders resummation of the perturbative contributions, and thus such derivations are not as rigorous as those for the meson form factors.[2,4]

In the case of hadron-hadron scattering amplitudes, some contributions to T_H have pinch singularities at finite values of the x_i -- corresponding to multiple quark-quark scattering at large momentum transfer with nearly on-shell intermediate states. However, these regions of integration are again suppressed by Sudakov form factors at the $q\bar{q}g$ vertices, and the hard-scattering region completely dominates the pinch contributions.[18] In fact, as conjectured by Mueller,[1] the leading contribution from these diagrams for meson-meson scattering arises from the region $|k_i^2| \sim \mathcal{O}(Q^2)^{1-\varepsilon}$ where $\varepsilon = (2c+1)^{-1}$, $c = 8C_F/(11 - 2/3\ n_f)$. [For four flavors, $\varepsilon \cong 0.281$.] In an Abelian theory where the Sudakov suppression is stronger, $|k_i^2| \sim \mathcal{O}(Q^2)$. Thus for meson-meson scattering at large momentum transfer we have

$$\mathcal{M}_{AB\to CD} = \int \left[dx_i\right] \phi_C^*\left(x_c, s_c, \tilde{Q}\right) \phi_D\left(x_d, s_d, \tilde{Q}\right) T_H\left(x_i, s_i, Q^2, \theta_{c.m.}\right) \times \phi_A\left(x_a, s_a, \tilde{Q}\right) \phi_B\left(x_b, s_b, \tilde{Q}\right) \quad . \tag{3.4}$$

The hard scattering amplitude T_H includes the Sudakov form factors which control and eliminate the pinch region. The effective value of $\tilde{Q}$ varies with the x_i phase-space integration. The leading power computed by Mueller for Eq. (3.4) is

$$\mathcal{M}_{\pi\pi\to\pi\pi} \sim \left(Q^2\right)^{-3/2 - c\,\ell n\,(2c+1)/2c} \cong \left(Q^2\right)^{-1.922} \tag{3.5}$$

compared to $(Q^2)^{-2}$ from dimensional counting.

Although detailed results for hadron-hadron scattering have not been completely worked out, we can abstract from the above analysis some general features of QCD common to all exclusive processes at large momentum transfer:

(1) All of the nonperturbative bound-state physics in the scattering amplitude is isolated in the process-independent distribution amplitudes. This is an essential feature of QCD factorization.

(2) Since the distribution amplitude ϕ is the $L_z = 0$ orbital angular momentum projection of the hadron wave function, the sum of the interacting constituents' spin along the hadron's momentum equals the hadron spin:

$$\sum_{i\varepsilon H} S_i^z = S_H^z \quad . \tag{3.6}$$

In contrast, there are any number of noninteracting spectator constituents in inclusive structure functions and the spin of the active quarks or gluons is only statistically related to the hadron spin in inclusive reactions (except at the edge of phase space $x \to 1$).

(3) Since all loop integrations in T_H are of order $\tilde{Q}$ the quark and hadron masses can be neglected at large Q^2 up to corrections of order $\sim m/\tilde{Q}$. The vector gluon coupling conserves quark helicity when all masses are neglected -- i.e., $\bar{u}_\downarrow \gamma^\mu u_\uparrow = 0$. Thus total quark helicity is conserved in T_H. In addition because of (2), the hadron's

helicity is the sum of the helicities of its valence quarks in T_H. We thus have the selection rule[19]

$$\sum_{\text{initial}} \lambda_H - \sum_{\text{final}} \lambda_H = 0 \quad , \tag{3.7}$$

i.e., total hadronic helicity is conserved, up to corrections of order m/Q or higher. Only flavor-singlet mesons in the 0^{-+} nonet can have a two-gluon valence component, and thus even for these states the quark helicity equals the hadronic helicity. Consequently hadronic helicity conservation applies for all amplitudes involving light mesons and baryons.[20] Exclusive reactions which involve hadrons with quarks or gluons in higher orbital angular states are suppressed by powers.

(4) The nominal power-law behavior of an exclusive amplitude at fixed $\theta_{c.m.}$ is $(1/Q)^{n-4}$ where n is the number of external elementary particles (quarks, gluons, leptons, photons, ...) in T_H. This dimensional counting rule[21] is modified by the Q^2-dependence of the factors of $\alpha_s(Q^2)$ in T_H, by the Q^2-evolution of the distribution amplitudes, and possibly by a small power correction associated with the Sudakov suppression of pinch singularities in hadron-hadron scattering. The dimensional counting rules in fact appear to be experimentally well-established for a wide variety of processes.

The helicity rule, Eq. (3.7), is one of the most characteristic features of QCD, being a direct consequence of the gluon's spin. A scalar or tensor gluon-quark coupling flips the quark's helicity. Thus, for such theories, helicity may or may not be conserved in any given diagram contributing to T_H, depending upon the number of interactions involved. Only for a vector theory, like QCD, can we have a helicity selection rule valid to all orders in perturbation theory.

The study of timelike hadronic form factors using e^+e^- colliding beams can provide very sensitive tests of this rule, since the virtual photon in $e^+e^- \to \gamma^* \to h_A\bar{h}_B$ always has spin ± 1 along the beam axis at high energies. Angular momentum conservation implies that the virtual photon can "decay" with one of only two possible angular distributions in the center of momentum frame: $(1+\cos^2\theta)$ for $|\lambda_A - \lambda_B| = 1$, and $\sin^2\theta$ for $|\lambda_A - \lambda_B| = 0$ where $\lambda_{A,B}$ are the helicities of hadron $h_{A,B}$. Hadronic helicity conservation, Eq. (3.7), as required by QCD greatly restricts the possibilities. It implies that $\lambda_A + \lambda_B = 0$ (since the photon carries no "quark helicity"), or equivalently that $\lambda_A - \lambda_B = 2\lambda_A = -2\lambda_B$. Consequently, angular momentum conservation requires $|\lambda_A| = |\lambda_B| = 1/2$ for baryons, and $|\lambda_A| = |\lambda_B| = 0$ for mesons; furthermore, the angular distributions are now completely determined:[19]

$$\begin{aligned} \frac{d\sigma}{d\cos\theta}\left(e^+e^- \to B\bar{B}\right) &\propto 1+\cos^2\theta \qquad \text{(baryons)} \\ \frac{d\sigma}{d\cos\theta}\left(e^+e^- \to M\bar{M}\right) &\propto \sin^2\theta \qquad \text{(mesons)} \end{aligned} \tag{3.8}$$

We emphasize that these predictions are far from trivial for vector mesons and for all baryons. For example, one expects distributions

like $1+\alpha\cos^2\theta$, $-1 < \alpha < 1$, in theories with a scalar or tensor gluon. So simply verifying these angular distributions [Eq. (3.8)] would give strong evidence in favor of a vector gluon.

The power-law dependence in s of these cross sections is also predicted in QCD, using the dimensional counting rule. Such "all orders" predictions for QCD allowed processes are summarized in Table I.[19] Processes suppressed in QCD are also listed there; these all violate hadronic helicity conservation, and are suppressed by powers of m^2/s in QCD. This would not necessarily be the case in scalar or tensor theories.

TABLE I

Exclusive channels in e^+e^- annihilation. The $h_A\bar{h}_B\gamma^*$ couplings in allowed processes are $-ie(p_A-p_B)^\mu F(s)$ for mesons, $-ie\bar{v}(p_B)\gamma^\mu G(s)u(p_A)$ for baryons, and $-ie^2\varepsilon_{\mu\nu\rho\sigma}p_M^\nu\varepsilon^\rho p_\gamma^\sigma F_{M\gamma}(s)$ for meson-photon final states. Similar predictions apply to decays of heavy-quark vector states, like the $\psi,\psi',\ldots$, produced in e^+e^- collisions.

	$e^+e^- \to h_A(\lambda_A)\,\bar{h}_B(\lambda_B)$	Angular Distribution	$\frac{\sigma(e^+e^- \to h_A\bar{h}_B)}{\sigma(e^+e^- \to \mu^+\mu^-)}$
Allowed in QCD	$e^+e^- \to \pi^+\pi^-, K^+K^-$	$\sin^2\theta$	$\frac{1}{4}\lvert F(s)\rvert^2 \sim c/s^2$
	$\rho^+(0)\rho^-(0), K^{*+}K^{*-}$	$\sin^2\theta$	$\frac{1}{4}\lvert F(s)\rvert^2 \sim c/s^2$
	$\pi^0\gamma(\pm1), \eta\gamma, \eta'\gamma$	$1+\cos^2\theta$	$(\pi\alpha/2)s\lvert F_{M\gamma}(s)\rvert^2 \sim c/s$
	$e^+e^- \to p(\pm\frac{1}{2})\bar{p}(\mp\frac{1}{2}), n\bar{n},\ldots$	$1+\cos^2\theta$	$\lvert G(s)\rvert^2 \sim c/s^4$
	$p(\pm\frac{1}{2})\bar{\Delta}(\mp\frac{1}{2}), \bar{n}\Delta,\ldots$	$1+\cos^2\theta$	$\lvert G(s)\rvert^2 \sim c/s^4$
	$\Delta(\pm\frac{1}{2})\bar{\Delta}(\mp\frac{1}{2}), y^*\bar{y}^*,\ldots$	$1+\cos^2\theta$	$\lvert G(s)\rvert^2 \sim c/s^4$
Suppressed in QCD	$e^+e^- \to \rho^+(0)\rho^-(\pm1), \pi^+\rho^-, K^+K^{*-},\ldots$	$1+\cos^2\theta$	$< c/s^3$
	$\rho^+(\pm1)\rho^-(\pm1),\ldots$	$\sin^2\theta$	$< c/s^3$
	$e^+e^- \to p(\pm\frac{1}{2})\bar{p}(\pm\frac{1}{2}), p\bar{\Delta}, \Delta\bar{\Delta},\ldots$	$\sin^2\theta$	$< c/s^5$
	$p(\pm\frac{1}{2})\bar{\Delta}(\pm\frac{3}{2}), \Delta\bar{\Delta},\ldots$	$1+\cos^2\theta$	$< c/s^5$
	$\Delta(\pm\frac{3}{2})\bar{\Delta}(\pm\frac{3}{2}),\ldots$	$\sin^2\theta$	$< c/s^5$

The exclusive decays of heavy quark atoms ($\psi,\psi',\ldots$) into light hadrons can also be analyzed in QCD.[22,16,19] The decay $\psi \to p\bar{p}$ for example proceeds via diagrams such as those in Fig. 4. Since ψ's produced in e^+e^- collisions must also have spin ±1 along the beam direction and since they can only couple to light quarks via gluons, all the properties listed in Table I apply to ψ, ψ', T, T',... decays as well. Already there is considerable experimental data for the ψ and ψ' decays.

Perhaps the most significant tests are the decays $\psi,\psi' \to p\bar{p}, n\bar{n},\ldots$. The predicted angular distribution $1+\cos^2\theta$ is consistent with published

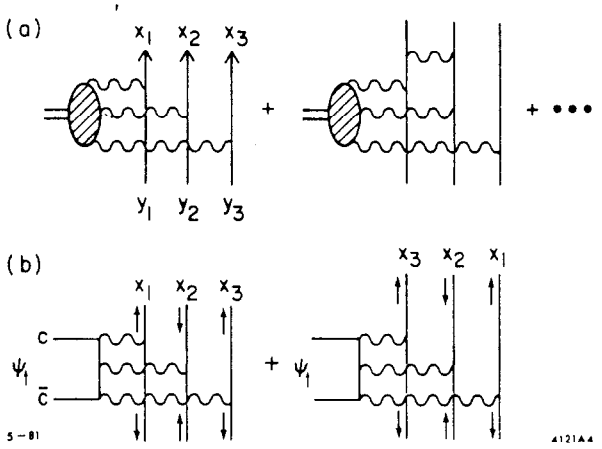

Fig. 4. (a) QCD analysis of $\psi \to B\bar{B}$. (b) Helicity-labeled, quark gluon subprocesses.

data.[16] This is important evidence favoring a vector gluon since scalar or tensor gluon theories would predict a distribution of $\sin^2\theta + \mathcal{O}(\alpha_s)$. Dimensional counting rules can be checked by comparing the ψ and ψ' rates into $p\bar{p}$, normalized by the total rates into light-quark hadrons so as to remove dependence upon the heavy-quark wave functions. Theory predicts[19]

$$\frac{BR(\psi \to p\bar{p})}{BR(\psi' \to p\bar{p})} \sim \left(\frac{M_{\psi'}}{M_{\psi}}\right)^8 \tag{3.9}$$

where

$$BR(\psi \to p\bar{p}) \equiv \frac{\Gamma(\psi \to p\bar{p})}{\Gamma(\psi \to \text{light-quark hadrons})} \quad . \tag{3.10}$$

Existing data suggests a ratio $(M_{\psi'}/M_{\psi})^n$ with $n \sim 8 \pm 3$, in good agreement with QCD.

Many more examples of exclusive reactions which test the basic scaling laws and spin structure of QCD are discussed in Refs. 2,7,19. The essential point is that exclusive reactions have the potential for isolating the QCD hard-scattering processes in situations where the helicities of all the interaction constituents are controlled. In contrast, in inclusive reactions the absence of restrictions on the spectator quark and gluons allows only a statistical correlation between the constituent and hadronic helicities.

IV. EXCLUSIVE TWO-PHOTON PROCESSES[15]

The two-photon reactions ($M = \pi, K, \rho, \omega, \ldots$)

$$\frac{d\sigma}{dt}(\gamma\gamma \to M\bar{M}) \qquad \text{at large } s = (k_1 + k_2)^2 \text{ and fixed } \theta_{c.m.}$$

provide a particularly important laboratory for testing QCD since these "Compton" processes are, by far, the simplest calculable large-angle exclusive hadronic scattering reactions. As we discuss below, the large-momentum-transfer scaling behavior, the helicity structure, and often even the absolute normalization can be rigorously computed for each two-photon channel.[13]

Conversely, the angular dependence of the $\gamma\gamma \to M\bar{M}$ amplitudes can be used to determine the shape of the process-independent meson "distribution amplitudes," $\phi_M(x,Q)$, the basic short-distance wavefunctions which control the valence quark distributions in high momentum transfer exclusive reactions.

A critically important feature of the $\gamma\gamma \to M\bar{M}$ amplitude is that the contributions of Landshoff pitch singularities are power-law suppressed at the Born level -- even before taking into account Sudakov form factor suppression. There are also no anomalous contributions from the $x \sim 1$ endpoint integration region. Thus, as in the calculation of the meson form factors, each fixed-angle helicity amplitude can be written to leading order in $1/Q$ in the factorized form [$Q^2 = p_T^2 = tu/s$; $\tilde{Q}_x = \min(xQ,(1-x)Q)$] (see Fig. 5):

$$\mathcal{M}_{\gamma\gamma \to M\bar{M}} = \int_0^1 dx \int_0^1 dy\ \phi_{\bar{M}}(y,\tilde{Q}_y)\, T_H(x,y,s,\theta_{c.m.})\, \phi_M(x,\tilde{Q}_x) \qquad (4.1)$$

where T_H is the hard-scattering amplitude $\gamma\gamma \to (q\bar{q})(q\bar{q})$ for the production of the valence quarks collinear with each meson and $\phi_M(x,Q)$ is the (process-independent) distribution amplitude for finding the valence q and $\bar{q}$ with light-cone fractions of the meson's momentum, integrated over transverse momenta $k_\perp < Q$. The contribution of nonvalence Fock states are power-law suppressed. Further, the spin-selection rule (3.7) of QCD predicts that vector mesons M and $\bar{M}$ are produced with opposite helicities to leading order in $1/Q$ and all orders in $\alpha_s(Q^2)$.

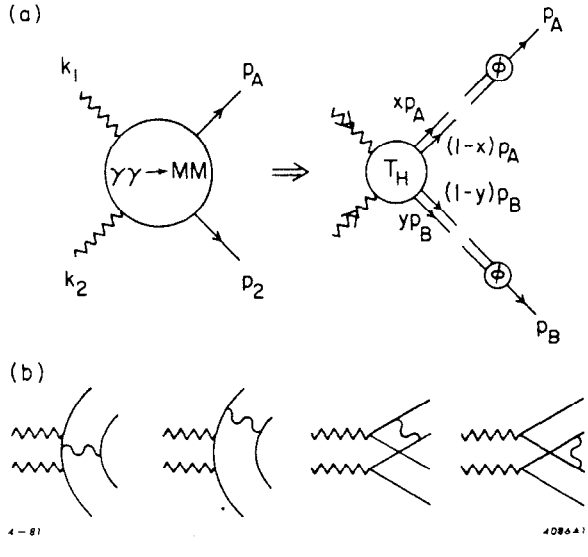

Fig. 5. (a) Factorized structure of the $\gamma\gamma \to M\bar{M}$ amplitude in QCD at large momentum transfer. The T_H amplitude is computed with quarks collinear with the outgoing mesons.
(b) Diagram contributing to T_H ($\gamma\gamma \to M\bar{M}$) to lowest order in α_s.

Dimensional counting[21] predicts that for large s, $s^4\, d\sigma/dt$ scales at fixed t/s or $\theta_{c.m.}$ up to factors of $\ell n\, s/\Lambda^2$.

Some forty diagrams contribute to the hard-scattering amplitudes for $\gamma\gamma \to M\bar{M}$ (for nonsinglet mesons). These can be derived from the four independent diagrams in Fig. 5b by particle interchange. The resulting amplitudes for helicity zero mesons are:

$$\left.\begin{matrix} T_{++} \\ T_{--} \end{matrix}\right\} = \frac{16\pi\alpha_s}{3s}\,\frac{32\pi\alpha}{x(1-x)y(1-y)}\left[\frac{(e_1-e_2)^2 a}{1-\cos^2\theta_{c.m.}}\right] \tag{4.2}$$

$$\left.\begin{matrix} T_{+-} \\ T_{-+} \end{matrix}\right\} = \frac{16\pi\alpha_s}{3s}\,\frac{32\pi\alpha}{x(1-x)y(1-y)}\left[\frac{(e_1-e_2)^2(1-a)}{1-\cos^2\theta_{c.m.}} + \frac{e_1e_2\,a(y(1-y)+x(1-x))}{a^2-b^2\cos^2\theta_{c.m.}}\right]$$

where $\left.\begin{matrix} a \\ b \end{matrix}\right\} = (1-x)(1-y) \pm xy$, the subscripts ++,--,... refer to photon helicities, and e_1, e_2 are the quark charges (i.e., the mesons have charges $\pm(e_1-e_2)$). To compute the $\gamma\gamma \to M\bar{M}$ amplitude $\mathcal{M}_{\lambda\lambda}$, (Eq. (4.1)), we now need only know the x-dependence of the meson's distribution amplitude $\phi_M(x,\tilde{Q})$; the overall normalization of ϕ_M is fixed by the 'sum rule' ($n_c = 3$)

$$\int_0^1 dx\, \phi_M(x,Q) = \frac{f_M}{2\sqrt{3}} \tag{4.3}$$

where f_M is the meson decay constant as determined from leptonic decays. Note that the dependence in x and y of several terms in $T_{\lambda\lambda}$, is quite similar to that appearing in the meson's electromagnetic form factor (2.10):

$$F_M(s) = \frac{16\pi\alpha_s}{3s}\int_0^1 dx\,dy\,\frac{\phi_M^*(x,\tilde{Q}_x)\;\phi_M^*(y,\tilde{Q}_y)}{x(1-x)\;y(1-y)} \tag{4.4}$$

when $\phi_M(x,Q) = \phi_M(1-x,Q)$ is assumed. Thus much of the dependence on $\phi(x,Q)$ can be removed from $\mathcal{M}_{\lambda\lambda}$, by expressing it in terms of the meson form factor — i.e.,

$$\left.\begin{matrix} \mathcal{M}_{++} \\ \mathcal{M}_{--} \end{matrix}\right\} = 16\pi\alpha\, F_M(s)\left[\frac{\langle(e_1-e_2)^2\rangle}{1-\cos^2\theta_{c.m.}}\right]$$

$$\left.\begin{matrix} \mathcal{M}_{+-} \\ \mathcal{M}_{-+} \end{matrix}\right\} = 16\pi\alpha\, F_M(s)\left[\frac{\langle(e_1-e_2)^2\rangle}{1-\cos^2\theta_{c.m.}} + 2\langle e_1e_2\rangle\; g\left[\theta_{c.m.};\phi_M\right]\right] \tag{4.5}$$

up to corrections of order α_s and m^2/s. Now the only dependence on ϕ_M, and indeed the only unknown quantity, is in the θ-dependent factor

$$g\left[\theta_{c.m.};\phi_M\right] = \frac{\int_0^1 dx\,dy \frac{\phi_M^*(x,\tilde{Q})\ \phi_M^*(y,\tilde{Q})}{x(1-x)\ y(1-y)} \frac{a\left[y(1-y)+x(1-x)\right]}{a^2 - b^2\cos^2\theta_{c.m.}}}{\int_0^1 dx\,dy \frac{\phi_M^*(x,\tilde{Q})\ \phi_M^*(y,\tilde{Q})}{x(1-x)\ y(1-y)}} \cdot \quad (4.6)$$

The spin-averaged cross section follows immediately from these expressions:

$$\frac{d\sigma}{dt} = \frac{2}{s}\frac{d\sigma}{d\cos\theta_{c.m.}} = \frac{1}{16\pi s^2}\frac{1}{4}\sum_{\lambda\lambda'}|\mathcal{M}_{\lambda\lambda'}|^2$$

$$= 16\pi\alpha^2\left|\frac{F_M(s)}{s}\right|^2\left\{\frac{\left\langle\left(e_1-e_2\right)^2\right\rangle^2}{\left(1-\cos^2\theta_{c.m.}\right)^2} + \frac{2\left\langle e_1e_2\right\rangle\left\langle\left(e_1-e_2\right)^2\right\rangle}{1-\cos^2\theta_{c.m.}}\right.$$

$$\left. \times\, g\left[\theta_{c.m.};\phi_M\right] + 2\left\langle e_1e_2\right\rangle^2 g^2\left[\theta_{c.m.};\phi_M\right]\right\} \quad . \quad (4.7)$$

In Fig. 6 the spin-averaged cross section (for $\gamma\gamma \to \pi\pi$) are plotted for several forms of $\phi_M(x,Q)$. At very large energies, the distribution amplitude evolves to the form

$$\phi_M(x,Q) \xrightarrow[Q\to\infty]{} \sqrt{3}\, f_M\, x(1-x) \quad , \quad (4.8)$$

and the predictions [curve (a)] become exact and parameter-free. However this evolution with increasing Q^2 is very slow (logarithmic), and at current energies ϕ_M could be quite different in structure, depending upon the details of hadronic binding. Curves (b) and (c) correspond to the extreme examples $\phi_M \propto [x(1-x)]^{1/4}$ and $\phi_M \propto \delta(x-\frac{1}{2})$, respectively. Remarkably, the cross section for charged mesons is essentially independent of the choice of ϕ_M, making this an essentially parameter-free prediction of perturbative QCD. By contrast, the predictions for neutral helicity-zero mesons are quite sensitive to the structure of ϕ_M. Thus we can study the x-dependence of the meson distribution amplitude by measuring the angular dependence of this process.

The cross sections shown in Fig. 6 are specifically for $\gamma\gamma \to \pi\pi$, where the pion form factor has been approximated by $F_\pi(s) \sim 0.4\ \text{GeV}^2/s$. The $\pi^+\pi^-$ cross section is quite large at moderate s:

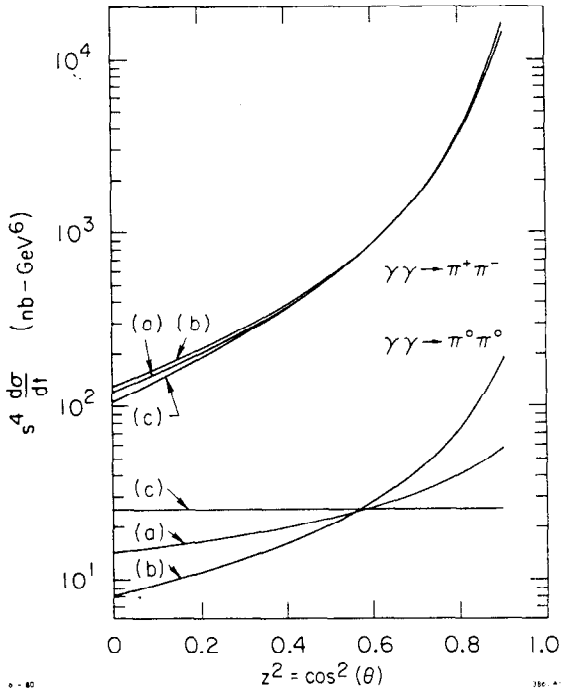

Fig. 6. QCD predictions for $\gamma\gamma \to \pi\pi$ to leading order in QCD. The results assume the pion form factor parameterization $F_\pi(s) \sim 0.4\ \text{GeV}^2/s$. Curves (a), (b) and (c) correspond to the distribution amplitudes $\phi_M = x(1-x)$, $[x(1-x)]^{\frac{1}{4}}$, and $\delta(x-\frac{1}{2})$, respectively. Predictions for other helicity zero mesons are obtained by multiplying with the scale constants given in Ref. 15.

$$\frac{\frac{d\sigma}{dt}(\gamma\gamma \to \pi^+\pi^-)}{\frac{d\sigma}{dt}(\gamma\gamma \to \mu^+\mu^-)} \sim \frac{4|F_\pi(s)|^2}{1-\cos^4\theta_{c.m.}} \sim \frac{0.6\ \text{GeV}^4}{s^2} \quad \text{at} \quad \theta_{c.m.} = \pi/2 \quad . \tag{4.9}$$

Similar predictions are possible for other helicity-zero mesons. The normalization of $\gamma\gamma \to M\bar{M}$ relative to the $\gamma\gamma \to \pi\pi$ cross section is completely determined by the ratio of meson decay constants $(f_M/f_\pi)^4$ and by the flavor-symmetry of the wave functions, provided only that ϕ_M and ϕ_π are similar in shape. Note that the cross section for charged ρ's with helicity zero is almost an order of magnitude larger than that for charged π's.

Finally notice that the leading order predictions [Eq. (4.5)] have no explicit dependence on α_s. Thus they are relatively insensitive to the choice of renormalization scheme or of a normalization scale. This is not the case for either the form factor or the two-photon annihilation amplitude when examined separately. However by combining the two analyses as in Eq. (4.5) we obtain meaningful results without computing $O(\alpha_s)$ corrections. The corresponding calculations for helicity one mesons are given in Ref. 13. Hadronic helicity conservation implies that only helicity-zero mesons can couple to a single highly virtual photon. So $F_{M_\perp}$, the transverse form factor cannot be measured experimentally. For simplicity we will assume that the longitudinal and transverse form factors are equal to obtain a rough estimate of the $\gamma\gamma \to \rho_\perp\rho_\perp$ cross section

(Fig. 7).[15] Again we see strong dependence on $\phi_{M_\perp}$ for all angles except $\theta_{c.m.} \sim \pi/2$, where the terms involving $g_\perp$ vanish. Consequently a measurement of the angular distribution would be very sensitive to the x-dependence of $\phi_{M_\perp}$, while measurements at $\theta_{c.m.} = \pi/2$ determine $F_{M_\perp}(s)$. Notice also that the number of charged ρ-pairs (with any helicity) is much larger than the number of neutral ρ's, particularly near $\theta_{c.m.} = \pi/2$. The cross sections are again quite large with

$$\left.\frac{d\sigma/dt\ (\gamma\gamma \to \rho_\perp^+ \rho_\perp^-)}{d\sigma/dt\ (\gamma\gamma \to \mu^+\mu^-)}\right|_{\theta_{c.m.} = \frac{\pi}{2}} \sim \frac{5\ \text{GeV}^4}{s^2} \quad . \tag{4.10}$$

Results for other mesons are given in Ref. 15.

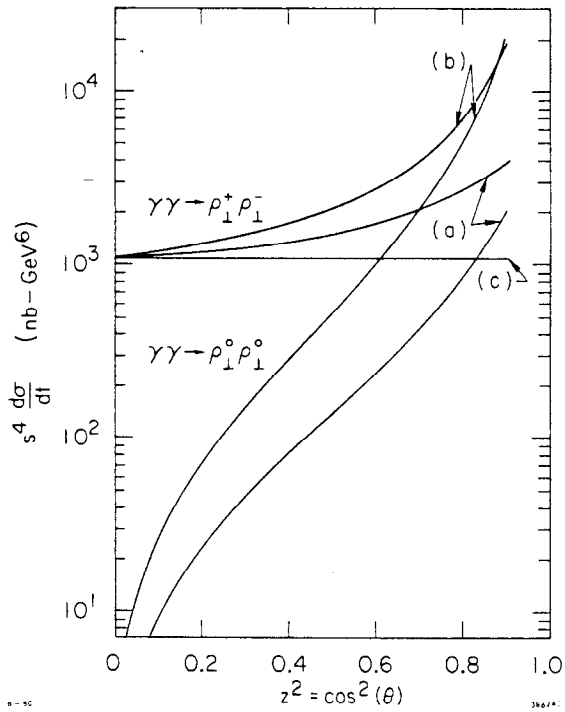

Fig. 7. QCD predictions for $\gamma\gamma \to \rho_\perp \bar{\rho}_\perp$ with opposite helicity ± 1 to leading order in QCD. The normalization given here assumes that the ρ distribution amplitude is helicity independent.

The $\gamma\gamma \to M\bar{M}$ and $\gamma^*\gamma \to M$ processes thus provide detailed checks of the basic Born structure of QCD, the scaling behavior of the quark and gluon propagators and interactions, as well as the constituent charges and spins. Conversely, the angular dependence of the $\gamma\gamma \to M\bar{M}$ amplitudes can be used to determine the shape of the process-independent distribution amplitude $\phi_M(x,Q)$ for valence quarks in the meson $q\bar{q}$ Fock state. The $\cos\theta_{c.m.}$-dependence of the $\gamma\gamma \to M\bar{M}$ amplitude determines the light cone x-dependence of the meson distribution amplitude in much the same way that the x_{B_j} dependence of deep inelastic cross sections determines the light-cone x-dependence of the structure functions (quark probability functions) $G_{q/M}(x,Q)$.

The form of the predictions given here are exact to leading order in $\alpha_s(Q^2)$. Power-law $(m/Q)^2$ corrections can arise from mass insertions, higher Fock states, pinch singularities and nonperturbative effects. In particular, the predictions are only valid when s-channel resonance effects can be neglected. It is likely that the background due to resonances can be reduced relative to the leading order QCD contributions if one measures the two-photon processes with at least one of the photons tagged at moderate spacelike momentum q^2, since resonance contributions are expected to be strongly damped by form factor effects. In contrast, the leading order QCD $\gamma_1\gamma_2 \to M\bar{M}$ amplitudes are relatively insensitive to the value of q_1^2 or q_2^2 for $|q_i^2| \ll s$.

Finally, we note that the amplitudes given above have simple crossing properties. In particular, we can immediately analyze the Compton amplitude $\gamma M \to \gamma M$ in the region t large enough with $s \gg |t|$ in order to study the leading Regge behavior in the large momentum transfer domain. In the case of helicity ± 1 mesons, the leading contribution to the Compton amplitude has the form ($s \gg |t|$)

$$\mathcal{M}_{\gamma M \to \gamma M} = 16\pi\alpha F_{M_1}(t)\left(e_1^2 + e_2^2\right) \qquad \left(\lambda_\gamma = \lambda'_\gamma\ ,\ \lambda_M = \lambda'_M\right) \tag{4.11}$$

which corresponds to a fixed Regge singularity at $J = 0$. In the case of helicity zero mesons, this singularity actually decouples, and the leading J-plane singularity is at $J = -2$.

V. APPLICATIONS TO HEAVY QUARK SYSTEMS

We can also use the above formalism for calculating exclusive amplitudes such as the decay of heavy quark systems into light hadrons. If we approximate the Ψ as a $|c\bar{c}\rangle$ bound state, then the lowest order amplitude for $\Psi \to p\bar{p}$ proceeds by the 3 gluon intermediate state shown in Fig. 4. The branching ratio is[19]

$$\frac{\Gamma(\psi \to 3g \to p\bar{p})}{\Gamma(\psi \to 3g \to \text{all})} = 3.2 \times 10^6\ \alpha_s^3(s)\ \frac{|\vec{P}_{CM}|}{\sqrt{s}}\ \frac{\langle T\rangle^2}{s^4} \tag{5.1}$$

where $|\vec{P}_{CM}|/\sqrt{s} \simeq .4$, $s = 9.6\ \text{GeV}^2$, and

$$\langle T\rangle \equiv \int_0^1 [dx][dy]\ \frac{\phi^*(y_i,s)}{y_1y_2y_3}\ \frac{x_1y_3 + x_3y_1}{[x_1(1-y_1) + y_1(1-x_1)][x_3(1-y_3) + y_3(1-x_3)]} \times \frac{\phi(x_i,s)}{x_1x_2x_3} \ . \tag{5.2}$$

Notice that there can be no endpoint singularities in the x_i and y_i integrations; the integrations are finite so long as $\phi(x_i,s) \lesssim Kx_i^{\epsilon}$ as $x_i \to 0$ for some $\epsilon > 0$. For this reason the present analysis is perhaps more reliable than that of the electromagnetic form factor. However, calculations of $\Gamma(\psi \to p\bar{p})$ cannot be carried beyond the first order corrections without a deeper understanding of the heavy-quark wave function. Still, the power-law behavior and hadronic helicity conservation are features valid to all orders and, given the uncertainties involved in analyzing heavy quark wave functions, they remain the most interesting aspects of this and similar decays. In addition, measurement of the $B\bar{B}$ branching ratios can be used as an important constraint on the normalization and shape of the baryon distribution amplitudes.

VI. RELATED QCD PROCESSES

The Fock state description of the hadron wavefunctions at equal-time on the light-cone allows a systematic study of a large number of QCD phenomena:

(a) The $x \to 1$ behavior of structure functions can be analyzed perturbatively. Only the minimal Fock state components contribute to the limiting behavior. The main power behavior corresponds to the spectator counting rule[23] with strong spin correlations. The perturbative QCD predictions reflect the elementary scaling of quark and gluon propagators in the far-off shell domain. A striking QCD prediction is that the helicity of the hadron tends to be carried by the constituent with the highest x.[24] The evolution of the structure functions must take into account the strong-phase limits at $x \to 1$. Detailed discussions of these results and the breakdown of the exclusive-inclusive correction are given in Ref. 24.

(b) The Fock state structure of QCD at infinite momentum is more complex than usually assumed in phenomenological applications. In addition to the "extrinsic" gluons generated by QCD evolution, there are always "intrinsic" gluons and non-valence quark components in the hadron wavefunction which are insensitive to the momentum scale of the probe.[25] For example, the $\lambda = \pm 1$ gluons exchanged between quarks, boosted to infinite momentum, yield an intrinsic gluon component to the Fock states. An even more striking example is the prediction[26] of "intrinsic charm" in the proton and meson wavefunctions. One can estimate,[27] using the bag model and perturbative QCD, that the proton bound state has a $|uudc\bar{c}\rangle$ component with a probability of ~1-2%. When this state is Lorentz boosted to infinite momentum, the constituents with the largest mass have the highest x. Thus heavy quarks (though rare) carry most of the momentum in the Fock state in which they are present. The usual parton model

assumption that non-valence sea quarks are always found at low x is incorrect. The diffractive dissociation of the proton's intrinsic charm state provides a simple explanation why charmed baryons and charmed mesons which contain no valence quarks in common with the proton are diffractively produced at large x_L with sizeable cross sections at ISR energies.[26,28]

(c) The irreducible Fock state wavefunctions of a hadron are strongly damped at $x \to 1$ and $x \to 0$, and thus do not yield non-singlet Regge behavior in the leading twist structure functions. If such Regge behavior exists it is specific to reducible nonperturbative corrections to the quark legs. A discussion will be given in Ref. 29.

(d) The distribution amplitude can be used to normalize higher twist (power-law suppressed) subprocesses in inclusive reactions. For example, one can compute a C/Q^2 contribution to the meson longitudinal structure function at large x from the $\gamma^* q\bar{q} \to q\bar{q}$ amplitude. This contribution is normalized to the meson distribution amplitude which in turn is normalized to the pion form factor.[30]

$$F_L^\pi(x,Q) = \frac{2x^2}{Q^2} C_F \int_{m^2/(1-x)}^{Q^2} dk^2 \, \alpha_s(k^2) \, F_\pi(k^2) \qquad (6.1)$$

which numerically is $F_L \sim x^2/Q^2$ (GeV^2 units).

The dominance of the longitudinal structure functions in the fixed W limit for mesons is an essential prediction of perturbative QCD. Perhaps the most dramatic consequence is in the Drell-Yan process $\pi p \to \ell^+\ell^- X$; one predicts[31] that for fixed pair mass Q, the angular distribution of the ℓ^+ (in the pair rest frame) will change from the conventional $(1+\cos^2\theta_+)$ distribution to $\sin^2(\theta_+)$ for pairs produced at large x_L. A recent analysis of the Chicago-Illinois-Princeton experiment[32] at FNAL appears to confirm the QCD high twist prediction with about the expected normalization. Striking evidence for the effect has also been seen in a Gargamelle analysis[33] of the quark fragmentation functions in $\nu p \to \pi^+\mu^- X$. The results yield a quark fragmentation distribution into positive charged hadrons which is consistent with the predicted form: $dN^+/dzdy \sim B(1-z)^2 + (C/Q^2)(1-y)$ where the $(1-y)$ behavior corresponds to a longitudinal structure function. It is also crucial to check that the $e^+e^- \to MX$ cross section becomes purely longitudinal ($\sin^2\theta$) at large z at moderate Q^2. Similarly one can absolutely normalize higher twist[34] (P_T^{-6}-scaling) amplitudes such as $qq \to Mq$ and $qq \to Mg$, which contribute strongly to $pp \to MX$ inclusive reactions at sub-asymptotic transverse momentum p_T. The corresponding analysis of γ induced reactions and $\gamma q \to Mq$ subprocesses is discussed in Ref. 35. The higher-twist amplitudes $\pi q \to gq$ and

$\pi g \to q\bar{q}$ lead to dramatic high p_T jet production processes where there is no hadron energy in the meson beam direction (see Ref. 36). Again, these cross sections can be absolutely normalized to the pion form factor.

(e) The Fock-state, light-cone perturbation theory methods allow a straightforward analysis of the effects of initial state hadronic interactions on QCD predictions for inclusive reactions such as the Drell-Yan reaction $p\bar{p} \to \mu^+\mu^- X$. As shown in Ref. 37, initial-state (Glauber) scattering severely disturbs the transverse momentum distributions of the interacting constituents. The $Q_\perp$ distribution of the dimuon pair is therefore not directly related to the intrinsic transverse momentum of the quarks in the hadronic wavefunction. Even more important, the color exchange between active quarks and spectator constituents in the hadron-hadron collisions leads to a non-trivial renormalization of the QCD factorization predictions, which however does not change the basic A^1 dependence of hadron-nucleus lepton-pair production processes at large Q^2. A detailed discussion will be given in Ref. 37.

(f) An important task is to further constrain the form and normalization of each Fock state wavefunction, especially for valence Fock states. A particularly interesting constraint is provided by the $\pi^0 \to 2\gamma$ decay amplitude in the $M_\pi^2 << R_\pi^{-2}$ limit. In a recent analysis with T. Huang, we obtain the constraint[38]

$$\int_0^1 dx\, \psi_{q\bar{q}}\,(k_\perp = 0, x) = \frac{\sqrt{n_c}}{f_\pi} \tag{6.2}$$

which can be interpreted as a constraint on the non-perturbative valence pion wavefunction at large distances. This result, plus the boundary condition (2.9) for the pion wavefunction at the origin, leads to the result that the probability of finding the $q\bar{q}$ state in the pion is $\leq \frac{1}{4}$, for a wide range of parameters of the $k_\perp$ and x dependence of $\psi_\pi(x,k_\perp)$. This result reinforces the argument that higher Fock states play an important role in the destruction of light hadrons. A discussion of the connection between rest frame and light-cone wavefunctions is also given in Ref. 38.

(g) Basic electromagnetic properties of hadrons such as low Q^2 form factors, magnetic moments, etc., can be defined in terms of the light-cone Fock state and wavefunctions. Detailed derivations are given in Refs. 2, 39. The analyses are inevitably complicated by the fact that the low Q^2 form factors receive contributions from all of the hadron Fock states, not just the valence $|q\bar{q}\rangle$ and $|qqq\rangle$ components.

(h) The methods used here have general applicability to atomic physics and nuclear physics problems. For example, the results discussed here for $\gamma\gamma^* \to \pi^0$ can be taken over immediately to $\gamma\gamma^* \to$ positronium with an obvious change of parameters. The value of Λ_{QCD} sets the approximate scale where a nuclear physics description in terms of hadronic degrees of freedom must merge with the QCD description in terms of quarks and gluons. It is also interesting to note that nuclear Fock states are much richer in QCD than they would be in a theory in which the only degrees of freedom are hadrons. For example, if we assume that at low relative momentum a deuteron is dominated by its usual n-p configuration, quark-quark scattering automatically generates color-polarized 6-quark states such as $|(uuu)_8(ddd)_8\rangle$ at short distances. The implications of QCD for large momentum transfer nuclear form factors and the nuclear force at short distances is discussed in Ref. 40.

(i) The fact that a meson can exist as a $|q\bar{q}\rangle$ state at small transverse separation implies that part of the time a meson will interact only weakly in nuclear targets. Such a state can be diffractively dissociated into q plus $\bar{q}$ jets at relatively large transverse momentum separation. A detailed discussion of such processes is given in Ref. 28.

ACKNOWLEDGEMENTS

We wish to thank E. Berger, G. Bodwin, S. Gupta, T. Huang, A. H. Mueller, and C. Peterson for helpful conversations, and to acknowledge the help and hospitality of D. Duke, J. Owens, and their colleagues at Florida State University.

REFERENCES

1. For recent reviews of perturbative QCD see A. H. Mueller, Columbia preprint CU-TP-192 (1981); A. J. Buras, Rev. Mod. Phys. 52, 1 (1980); E. Reya, Phys. Rept. 69, 195 (1981); S. J. Brodsky and G. P. Lepage, SLAC-PUB-2447, 1979 SLAC Summer Institute.
2. G. P. Lepage and S. J. Brodsky, Phys. Rev. D22, 2157 (1980); Phys. Lett. 87B, 359 (1979), and references therein.
3. A. V. Efremov and A. V. Radyushkin, Rev. Nuovo Cimento 3, 1 (1980); Phys. Lett. 94B, 245 (1980) and references therein.
4. A. Duncan and A. Mueller, Phys. Rev. D21, 1636 (1980); Phys. Lett. 98B, 159 (1980). A. H. Mueller, Ref. 2.

5. See also G. R. Farrar and D. R. Jackson, Phys. Rev. Lett. 43, 246 (1979); V. L. Chernyak and A. R. Vhitnishii, JETP Lett. 25, 11 (1977); G. Parisi, Phys. Lett. 43, 246 (1979); M. K. Chase, Nucl. Phys. B167, 125 (1980).
6. For earlier reviews of these topics see S. J. Brodsky and G. P. Lepage, SLAC-PUB-2294, 2447, 2605, and 2656, and A. Mueller, Ref. 2.
7. For a discussion of possible complications due to confinement effects see S. Gupta and H. Quinn, to be published.
8. See S. J. Brodsky, T. Huang, and G. P. Lepage, SLAC-PUB-2540 (1980), and references therein. The light-cone perturbation theory rules are given in Ref. 2, and references therein.
9. S. J. Brodsky and G. P. Lepage, Ref. 1.
10. S. J. Brodsky, Y. Frishman, G. P. Lepage, and C. Sachrajda, Phys. Lett. 91B, 239 (1980). See also A. Duncan and A. Mueller, Ref. 4, and M. K. Chase, Ref. 5.
11. R. D. Field, R. Gupta, S. Otto, and L. Chang, University of Florida preprint 80-21; R. Gupta, CALT-68-946 and these proceedings. See also F. M. Dittes and A. V. Radyushkin, Dubna preprint JINR-E2-80-688 (1980).
12. S. J. Brodsky, Y. Frishman, and G. P. Lepage (in progress).
13. S. J. Brodsky and G. P. Lepage, SLAC-PUB-3733 (1981).
14. P. V. Landshoff, Phys. Rev. D10, 1024 (1974); P. Cvitanovic, Phys. Rev. D10, 338 (1974); S. J. Brodsky and G. Farrar, Phys. Rev. D11, 1309 (1975).
15. S. J. Brodsky and G. P. Lepage, Ref. 13, and SLAC-PUB-2587 (1980) presented at the XXth International Conference on High Energy Physics, Madison.
16. S. Gupta, SLAC-PUB-2653 (1980).
17. S. J. Brodsky, G. P. Lepage, and S.A.A. Zaidi, Phys. Rev. D23, 1152 (1981). S. J. Brodsky and G. P. Lepage, Phys. Rev. Lett. 43, 545 (1979), Erratum ibid. 43, 1625 (1979). See also Ref. 4.
18. P. V. Landshoff and D. J. Pritchard, Z. Phys. C6, C9 (1980). G. P. Lepage and S. J. Brodsky, Ref. 2.
19. S. J. Brodsky and G. P. Lepage, SLAC-PUB-2656 (1980), presented at the International Symposium on High Energy Physics with Polarized Beams and Polarized Targets, Lausanne (1980). S. J. Brodsky and G. P. Lepage, SLAC-PUB-2746 (1980).
20. Arguments for the conservation of baryon chirality in large momentum transfer processes have been given by B. L. Ioffe, Phys. Lett. 63B, 425 (1976). For some processes this rule leads to different predictions than the QCD results given here.
21. S. J. Brodsky and G. R. Farrar, Phys. Rev. Lett. 31, 1153 (1973), and Phys. Rev. D11, 1309 (1975); V. A. Matveev, R. M. Muradyan and A. V. Tavkheldize, Lett. Nuovo Cimento 7, 719 (1973).
22. A. Duncan and A. H. Mueller, Phys. Lett. 93B, 119 (1980).
23. R. Blankenbecler and S. J. Brodsky, Phys. Rev. D10, 2973 (1974).
24. See S. J. Brodsky and G. P. Lepage, SLAC-PUB-2447 (1979), SLAC-PUB-2605 (1980), Ref. 19, and references therein.
25. S. J. Brodsky and J. F. Gunion, Phys. Rev. D19, 1005 (1979).

26. S. J. Brodsky, P. Hoyer, C. Peterson, and N. Sakai, Phys. Lett. 93B, 451 (1980), and S. J. Brodsky, C. Peterson, and N. Sakai, Phys. Rev. D23, 2745 (1981).
27. J. F. Donoghue and E. Golowich, Phys. Rev. D15, 3421 (1977).
28. G. Bertsch, S. J. Brodsky, A. H. Goldhaber, and J. F. Gunion, preprint NSF-ITP-81-23/SLAC-PUB-2748 (1981).
29. S. J. Brodsky, T. Huang, and G. P. Lepage (in preparation).
30. E. L. Berger, S. J. Brodsky, and G. P. Lepage (in preparation), S. J. Brodsky and G. P. Lepage, SLAC-PUBs 2601 and 2605. See also G. R. Farrar and D. R. Jackson, Phys. Rev. Lett. 35, 1416 (1975).
31. E. L. Berger and S. J. Brodsky, Phys. Rev. Lett. 42, 940 (1979). E. L. Berger, Phys. Lett. 89B, 241 (1980), Z. Phys. C4, 289 (1980).
32. K. J. Anderson et al., Phys. Rev. Lett. 43, 1219 (1979).
33. CERN-MILAN-ORSAY Collaboration, CERN-EP/80-124 (1980); C. Matteuzzi et al., contributed to the XXth International Conference on High Energy Physics, Madison, Wisconsin, July 17-23, 1980.
34. E. L. Berger, T. Gottschalk, D. Sivers, Phys. Rev. D23, 99 (1981). See also G. Farrar and G. C. Fox, Nucl. Phys. B167, 205 (1980).
35. J. Bagger and J. F. Gunion (to be published). S. J. Brodsky, J. F. Gunion, R. Rückl, Phys. Rev. D18, 2469 (1978).
36. E. L. Berger and S. J. Brodsky, ANL-HEP-PR-81-14/SLAC-PUB-2449 (1981).
37. G. Bodwin, S. J. Brodsky, and G. P. Lepage (in preparation).
38. S. J. Brodsky, T. Huang, and G. P. Lepage, SLAC-PUB-2540 (1980).
39. S. J. Brodsky and S. D. Drell, Phys. Rev. D22, 2236 (1980).
40. S. J. Brodsky and G. P. Lepage, SLAC-PUB-2595, published in the Proceedings of the IXth International Conference on the Few Body Problem, Eugene, Oregon (1980); S. J. Brodsky and B. T. Chertok, Phys. Rev. Lett. 37, 279 (1976) and Phys. Rev. D14, 3003 (1976).